QUANTIFICATION OF LYMPHATIC VASCULAR

PERMEABILITY VIA NEAR-INFRARED IMAGING

A Thesis
Presented to
The Academic Faculty

by

Mindy Ross

In Partial Fulfillment
of the Requirements for the Degree
B.S. in Biochemistry with the Research Option in the
School of Chemistry and Biochemistry

Georgia Institute of Technology
May 2017

QUANTIFICATION OF LYMPHATIC VASCULAR

PERMEABILITY VIA NEAR-INFRARED IMAGING

Approved by:

Dr. J. Brandon Dixon, Advisor
George W. Woodruff School of Mechanical
Engineering
Georgia Institute of Technology

Dr. Levi Wood
George W. Woodruff School of Mechanical
Engineering
Georgia Institute of Technology

Date Approved: April 28, 2017

ACKNOWLEDGEMENTS

I would like to thank the members of my lab, especially Tyler Nelson and my research professor J. Brandon Dixon, for guiding me throughout my project.

TABLE OF CONTENTS

LIST OF FIGURES

LIST OF ABBREVIATIONS

PEG	Methoxypoly(ethylene glycol)
NIR	Near-Infrared
ROI	Region of Interest
IFN-γ	Interferon-γ
P_s	Apparent Vessel Permeability

SUMMARY

Though the lymphatic system is involved in many essential bodily functions, little is known about its role in the progression of lymphatic diseases like lymphedema. Recently, inflammation has been implicated as the primary mediator of lymphatic pathologies, due to its ability to decrease lymphatic function and induce a mal-adaptive remodeling response (Aldrich & Sevick-Muraca, 2013). One of the failure modes that inflammation is hypothesized to influence is by increasing the permeability of the lymphatic vasculature (Scallan & Huxley, 2010). A minimally-invasive method of quantifying lymphatic vessel permeability was designed using near-infrared imaging, a fluorescent tracer, and applied pressure. The method partially occluded the lymphatic collecting vessels and was tested using IFN-γ as a positive control. The average apparent permeability for the control group was determined to be somewhat similar to a previous *in vivo* study of isolated vessels but had a wide range of values overall (Scallan & Huxley, 2010). Comparison of the IFN-γ treated group to the control group revealed no significant difference and therefore inconclusive results as to the accuracy of the method. Future work will include testing different positive controls to verify the method followed by application of the method on diet-induced obese mice for determination of the changes to vessel permeability as compared to the control group to understand possible causes that contribute to the development of lymphatic diseases like lymphedema.

CHAPTER 1

INTRODUCTION

The lymphatic system is a network of vessels, nodes, and accessory organs that serves many essential biological functions. Most notably the lymphatic system is responsible for immune cell trafficking, absorbing and transporting lipids from the digestive system, and restoring fluids extravagated from the circulatory system. Despite these essential functions, little is known about the role of the lymphatics in the progression of a variety of diseases. Previous studies have identified changes in the lymphatic vasculature characteristic of lymphedema to include dermal backflow, dilated lymphatic vessels, and decreased effective pumping pressure (Unno *et al.*, 2007; Nelson *et al.*, 2014). However, the causes of the changes to the lymphatic system that result in dysfunction still need to be investigated before a cure can be developed. A novel technique being developed is near-infrared (NIR) imaging, which uses a fluorescent dye to image the lymphatic vessel in real time (Rasmussen *et al.*, 2009). This technique has the potential to serve as a new diagnostic tool for lymphatic diseases like lymphedema; it could significantly improve the lives of the individuals affected by providing early detection of the abnormalities in the lymphatic system and facilitating immediate treatment.

Using fluorescence imaging, previous research has been conducted to assess the permeability of the lymphatic vessel *in vivo* (Scallan & Huxley, 2010). However, changes to lymphatic permeability that occur due to inflammation have yet to be determined using a minimally invasive *in vivo* method. The current experiment expands on previous studies by developing a minimally invasive method of quantifying permeability *in vivo* in order to assess the changes that occur due to inflammation as seen in lymphedema patients. The results of this

study contribute a methodology to a better understanding of the lymphatic system, which could ultimately accelerate the development of treatment options to reverse the symptoms of lymphatic disease.

CHAPTER 2

LITERATURE REVIEW

The lymphatic system has become increasingly popular in current studies due to the growing prevalence of lymphatic disease in the population. One of these diseases is secondary lymphedema, which is an acquired lymphatic disease characterized by swelling of the affected limb and fluid stagnation that can occur as a result of breast cancer treatment in addition to other causes (Morrell *et al.*, 2005). Currently, lymphedema has no cure, and the success of the treatment options varies depending on the individual and stage at which the disease is detected (Cheifetz *et al.*, 2010). Studies have estimated that the incidence of breast cancer-related lymphedema is approximately 12%, but the various detection methods currently available such as circumferential methods and self-reporting have led to many undetected cases and false diagnoses (Hayes *et al.*, 2008; Thomas-Maclean *et al.*, 2008). These techniques also are ineffective in the early stages of the disease, so magnetic resonance imaging (MRI), computed tomography (CT), and lymphoscintigraphy have been utilized for improved early diagnosis and thus more effective treatment of the disease due to the ability to assess lymphatic function and dysfunction (Mihara *et al.*, 2012).

A novel technique being developed is near-infrared (NIR) imaging, which is a minimally invasive technique that uses a fluorescent dye optimized for uptake by the lymphatics to image the lymphatic system in real time (Rasmussen *et al.*, 2009). When this technique was compared to the other imaging methods currently in use, Mihara and colleagues found that NIR imaging was the superior method in terms of sensitivity to determine changes in the lymphatic system due to the onset of lymphatic disease (Mihara *et al.*, 2012). Currently, the fluorescent dye used to

image the lymphatic vessels is indocyanine green (ICG), since it has already been FDA approved for use in other diagnostic techniques. However, previous studies have shown that ICG adversely affects lymphatic function (Weiler & Dixon, 2013). As a result, the dye LI-COR IRDye 800CW NHS ester was conjugated to a PEG amine by a modified protocol described by Proulx and colleagues for studies involving the quantification of lymphatic properties with NIR imaging to avoid confounding the results with the effect of the dye on lymphatic function (Proulx *et al.*, 2013).

In order to better understand how lymphedema occurs, a more detailed understanding is needed of the changes in the lymphatic vasculature that result in dysfunction. Previous studies have found that obesity can increase the risk of the development of lymphedema after breast cancer treatment (Treves, 1957). In addition, obesity alone was found to be a potential cause of the development of lymphedema through the comparison of two groups of individuals with varying body mass indexes in a study conducted by Greene and colleagues (Greene *et al.*, 2015). The correlation between obesity and lymphatic disease could be due to the chronic inflammation present in obese individuals. Our lab has demonstrated that nitric oxide, which is released during inflammation, causes impaired function of the affected lymphatic vessels seen through reduced fluid transport (Weiler *et al.*, 2012). Inflammation has also been implicated to cause increased vessel permeability, which could contribute to the development of lymphatic dysfunction (Scallan & Huxley, 2010). However, studies have yet to develop minimally invasive methods to analyze the effect of inflammation on lymphatic vessel permeability due to the previous difficulty of imaging fluid transport through the lymphatic vessel in real time.

This study aims to use NIR imaging in combination with the LI-COR IRDye 800CW NHS ester to develop a minimally invasive technique to quantify lymphatic vessel permeability

in vivo by combining and modifying previously described techniques of dye infusion at constant pressure with permeability calculations (Swartz & Boucher, 1999; Scallan & Huxley, 2010). The method will then be utilized for future studies in models of diet-induced obesity to observe the changes that occur to lymphatic vessel permeability as a result of chronic inflammation induced by obesity. C57BL/6 mice have been chosen as the obesity model due to previous studies showing their susceptibility to obesity while on a high-fat diet, which resulted in up-regulation of pro-inflammatory cytokines in adipose tissues (Montgomery *et al.*, 2013). Comparison of the lymphatic vessel permeability in obese C57BL/6 mice to that of BALB/c mice, which have been shown to have some resistance to obesity, will reveal the changes to the lymphatic vasculature caused by chronic inflammation that result in lymphatic dysfunction (Montgomery *et al.*, 2013; Savetsky *et al.*, 2014). By having a better understanding of the effects of chronic inflammation on the lymphatic system, the findings of this study will contribute towards the long-term goal of the development of treatment options that are able to reverse the symptoms of lymphedema.

CHAPTER 3

MATERIALS AND METHODS

Synthesis of PEG-IRDye

Methoxypoly(ethylene glycol) (PEG) amine (13kDa, 15nmol) was dissolved in anhydrous DMSO with heat. The PEG molecules were labeled with LI-COR IRDye 800CW NHS ester (LI-COR Biosciences, Lincoln, NE) predissolved in anhydrous DMSO (8.57nmol) at room temperature for 48 hours. The crude dye solution was purified for 48 hours using Slide-A-Lyzer^{TM} Dialysis Cassettes (Thermo Fisher Scientific, Rockford, IL) then lyophilyzed overnight. The freeze-dried product stored at -20˚C was reconstituted in double-distilled water (40μL) prior to use.

Fluorescence Image Capture via Near-Infrared Imaging

Lymphatic vessel permeability was quantified in the tail of six-month-old female BALB/c mice (Charles River Laboratories, Wilmington, MA) in accordance with procedures approved by the Georgia Institute of Technology IACUC Review Board. Mice were anesthetized with 5% isoflurane for about 10 minutes. After the anesthetic had taken effect, mice were kept on about 1.5% isoflurane for the rest of the experiment and positioned under the camera either on its stomach or on its side so that the field of view was 2 cm from the base of the tail. A pressure cuff connected to a pressure cuff controller and a custom-made LabView program previously developed in the lab was positioned proximal to the field of view with only the edge of the cuff visible (Nelson *et al.*, 2014). The magnification on the camera was set to 1.25X with a camera exposure time of 50ms, and the percent light transmittance was adjusted to 8% using neutral

density filters. The PEG-IRDye (0.25mg/mL, 10μL) was injected intradermally into the tip of the mouse tail. Image acquisition of the lymphatic vessels using a custom NIR lymphatic imaging device and LabView program developed previously by the lab (Weiler *et al.*, 2012) began just before injection at a rate of 1fps and lasted for 15 minutes. Once fluorescence was seen in the lymphatic collecting vessels, the pressure cuff was applied at 60mmHg and held constant until the end of the image acquisition to partially occlude the lymphatic vessels and encourage fluid leakage from the vessels.

Image Processing

Fluorescence measurements were taken in the region of interest (ROI) to include either the region between the two lymphatic vessels or around one lymphatic vessel and surrounding tissue in the mouse tail using ImageJ software to quantify the fluorescence intensities (NIH, Bethesda, MD). The fluorescence intensity was plotted over time, and the change in fluorescence intensity over time was determined using a linear regression.

Calculation of Apparent Vessel Permeability

Calculation of the apparent vessel permeability (P_s, cm s^{-1}) was done using an equation derived by Scallan and colleagues that linked the change in fluorescence intensity over time (dI_f/dt) in the region of interest after application of the pressure cuff at 60mmHg to the volume-to-surface area ratio ($D/4$). The diameter of the lymphatic collecting vessel was estimated to be 25μm. The intensity values were normalized using the initial fluorescence intensity value (I_o) (Scallan & Huxley, 2010).

$$P_s = \left(\frac{1}{I_o}\right)\left(\frac{dI_f}{dt}\right)\left(\frac{D}{4}\right)$$
(Scallan & Huxley, 2010)

<u>Treatment of IFN-γ</u>

Three hours prior to imaging, mice were anesthetized with 5% isoflurane for about 10 minutes. After the anesthetic had taken effect, the mice were maintained on about 1.5% isoflurane for injection of IFN-γ in sterile PBS (1μg/mouse) at the tip of the tail intradermally until after treatment. Image capture was performed identically to the control group with the ROI between the two lymphatic vessels only.

CHAPTER 4

RESULTS

The NIR imaging conditions were optimized to prevent photobleaching of the fluorescent dye. NIR imaging of the region of interest over time was used to track the movement of the injected tracer through the lymphatic collecting vessel and surrounding interstitium. The change in fluorescence intensity over time was measured between the two lymphatic vessels (Figure 1) and around one vessel for the control group (Figure 2). The dye was seen to leak into the surrounding tissue from the collecting vessel over time.
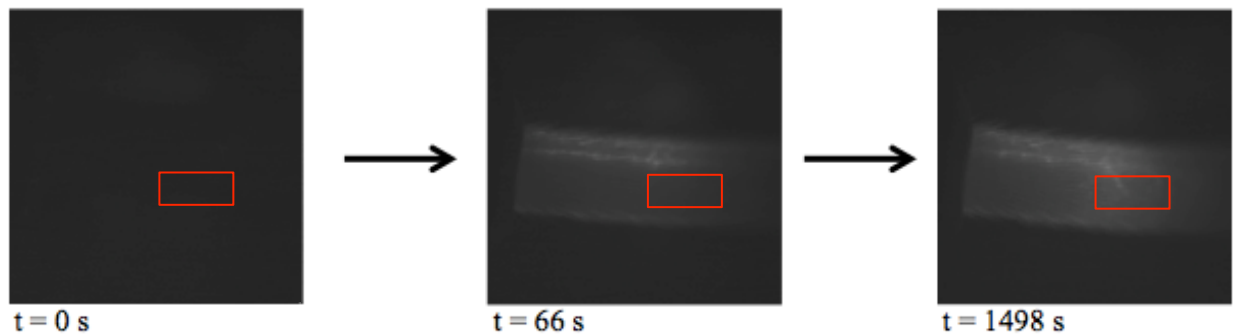

t = 0 s   t = 66 s   t = 1498 s

Figure 1. Images over time of a mouse tail distal to an occlusion cuff at a pressure of 60mmHg after a 13kDa fluorescent dye was injected intradermally into the tip of the tail with the region of interest shown by the red box.

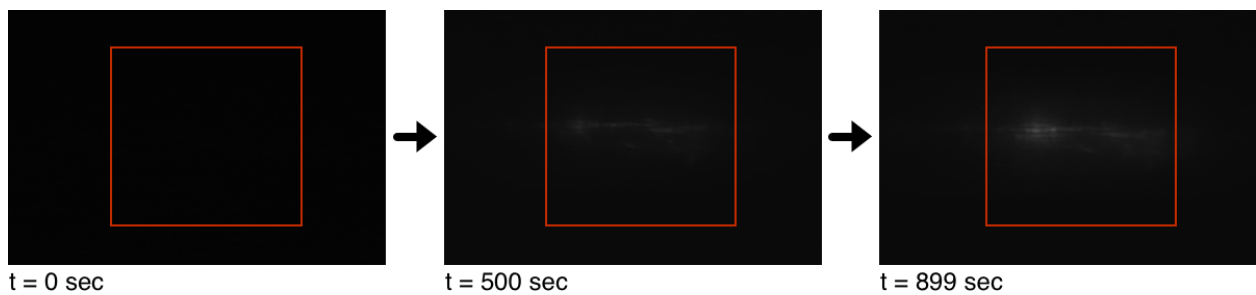t = 0 sec   t = 500 sec   t = 899 sec

Figure 2. Images of the side of the mouse tail over time after injection of the fluorophore to show the accumulation of fluorescence in the region of interest (red box) after partial vessel occlusion.

The fluorescence intensity in the ROI was quantified and plotted over time to determine the overall change in fluorescence intensity (Figures 3-4).
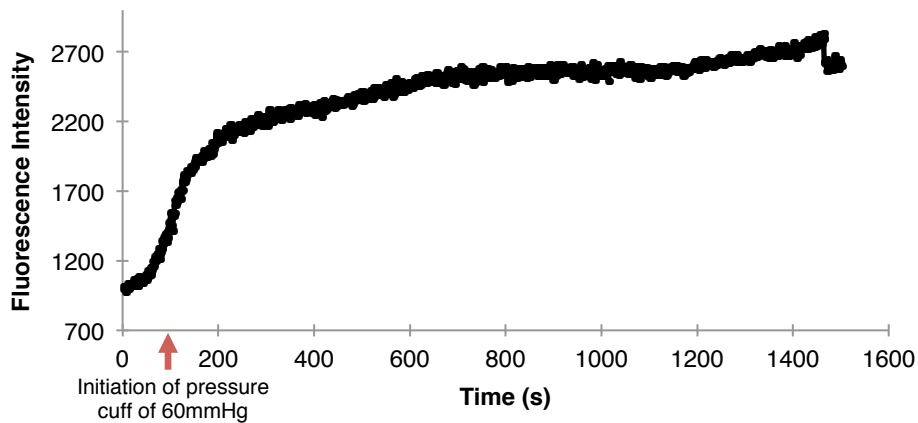
Figure 3. Quantification of the fluorescence intensity over time in the region of interest between the two collecting lymphatic vessels of the mouse tail. Pressure (60 mmHg) to occlude the lymphatic vessels was applied to the tail after 110 seconds.
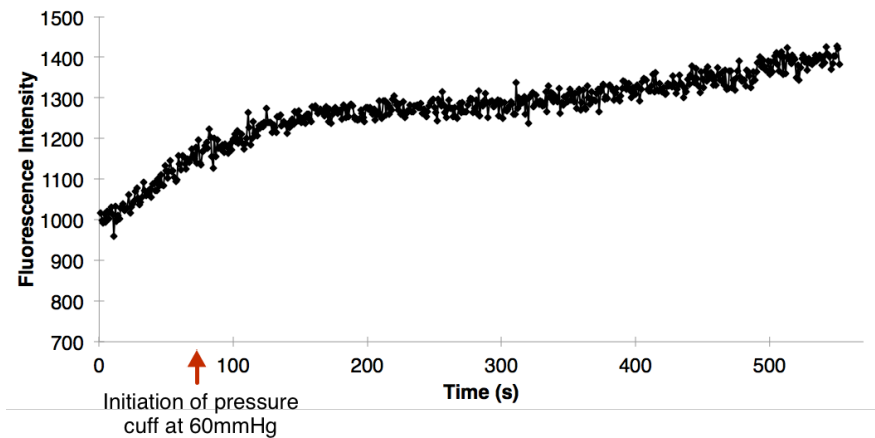

Figure 4. Plot of the fluorescence intensity when the ROI was around one lymphatic vessel as a function of time showing the gradual increase in fluorescence due to dye accumulation in the interstitial tissue around the lymphatic collecting vessel after pressure (60 mmHg) was applied after 80 seconds.

Apparent permeability was calculated using the equation derived by Scallan and colleagues and determined to be $8.08 \times 10^{-6} \pm 9.71 \times 10^{-6}$ cm s^{-1} when the ROI was between the two lymphatic vessels and $6.09 \times 10^{-6} \pm 6.08 \times 10^{-6}$ cm s^{-1} when the ROI was around one lymphatic vessel (Scallan & Huxley, 2010).

To determine the effect of induced inflammation on lymphatic vessel permeability, mice were treated locally with IFN-γ prior to imaging. The change in fluorescence intensity over time was tracked and plotted, as shown in Figure 5.
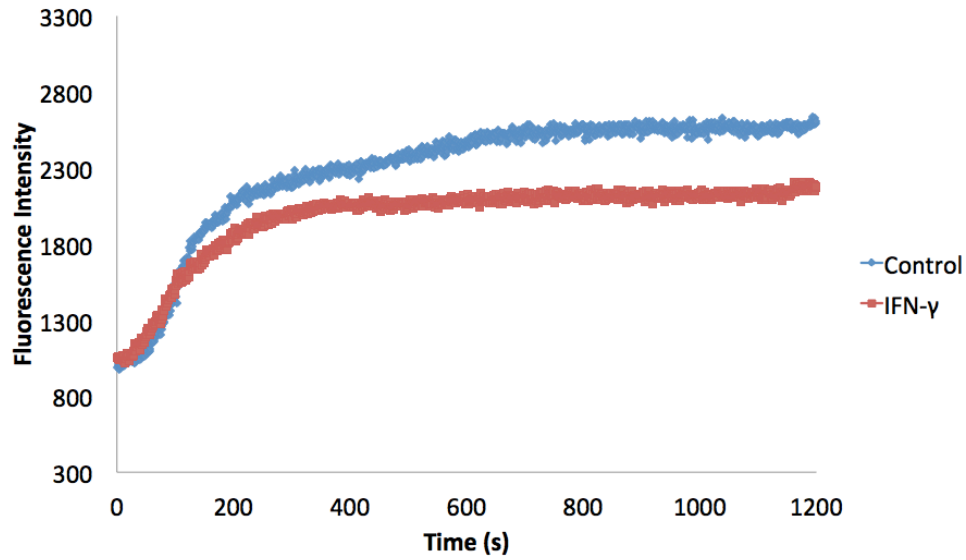
Figure 5. Plot of the fluorescence intensity over time in the ROI between the two lymphatic vessels with and without treatment of IFN-γ. Pressure (60 mmHg) to partially occlude the lymphatic vessels was applied after fluorescence was seen in the ROI.

The apparent permeability of the IFN-γ treated group was compared to the control and found to be a nonsignificant difference after evaluation by a Student's T-Test to obtain a p-value of 0.135 (Figure 6).
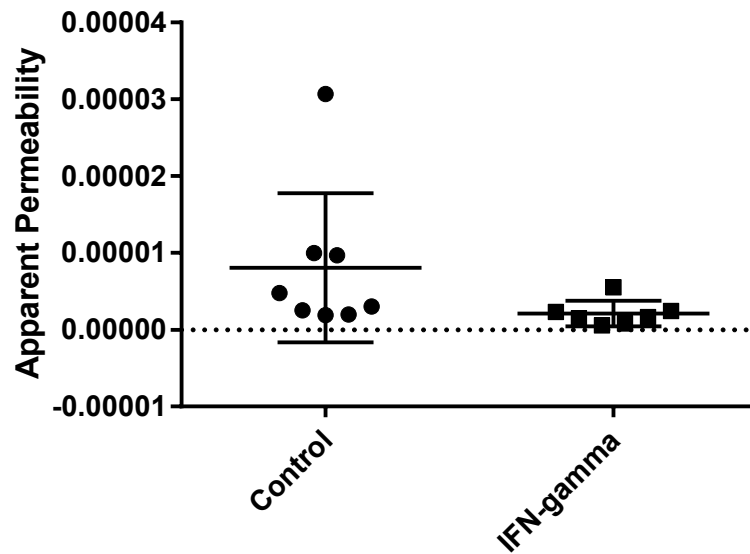

Figure 6. Comparison of the average apparent vessel permeability for the control and IFN-γ treated groups with corresponding error bars.

CHAPTER 5

DISCUSSION

Imaging of the fluorescent tracer through the lymphatic collecting vessel showed an initial increase in fluorescence intensity as the dye entered the ROI followed by a gradual increase correlating to the dye accumulated in the vessel and surrounding tissue for most trials, as shown in Figures 1-4. Secondary collecting vessels in parallel were seen in some animals to assist in fluid transport through the tail. Overall, partial occlusion of the lymphatic collecting vessels at 60 mmHg was sufficient to promote dye leakage through the vessel walls into the surrounding tissue. The calculated average apparent vessel permeability in the control group using both imaging methods was somewhat similar to a previous *in vivo* study of isolated vessels but had a wide range of values overall, shown by the large standard deviation (Scallan & Huxley, 2010).

The increase in fluorescence intensity in the lymphatic vessels of the IFN-γ treated group followed a similar trend to the control group. The initial increase in the fluorescence intensity in the ROI following injection of the tracer was more gradual than that of the control group for most trials. The average apparent permeability in the control group was compared to that of the IFN-γ treated group to verify the imaging method for quantification of vessel permeability, since IFN-γ was thought to increase the permeability of the lymphatic vessels. The apparent vessel permeability in the IFN-γ treated group was opposite of what was expected and was smaller than the calculated average apparent permeability of the control group. However, the difference in the apparent permeabilities was not significant as shown by the p-value of 0.135, suggesting that

12

IFN-γ did not increase the permeability of the lymphatic vessels or that the designed method was

not adequate to quantify lymphatic vessel permeability using the fluorescent tracer.

CHAPTER 6

CONCLUSION AND FUTURE WORK

A minimally-invasive method for quantification of lymphatic vessel permeability *in vivo* was designed for determination of the role that vessel permeability plays in the progression of lymphedema. This technique was then tested using the positive control IFN-γ to verify its accuracy. There was a non-significant difference between the control group and IFN-γ treated groups and the lower calculated average P_s of the IFN-γ treated group than the control group, which questions the accuracy of the method or the validity of the positive control. Future work will include testing different positive controls known to increase lymphatic vessel permeability for verification of the method for quantification of vessel permeability. Once the method has been established, the apparent lymphatic vessel permeability in models of diet-induced obesity will be calculated to compare to the control for determination of any changes to vessel permeability, since obesity is a major risk factor for the development of lymphedema and can worsen the symptoms (Treves, 1957; Greene *et al.*, 2015). The results of this study will contribute to the knowledge about the progression of lymphedema and to the development of novel treatment options to improve the lives of those afflicted.

REFERENCES

Aldrich MB & Sevick-Muraca EM. (2013). Cytokines are systemic effectors of lymphatic function in acute inflammation. *Cytokine* **64,** 362-369.

Cheifetz O, Haley L & Breast Cancer A. (2010). Management of secondary lymphedema related to breast cancer. *Canadian Family Physician* **56,** 1277-1284.

Greene AK, Grant FD, Slavin SA & Maclellan RA. (2015). Obesity-induced lymphedema: clinical and lymphoscintigraphic features. *Plastic and reconstructive surgery* **135,** 1715-1719.

Hayes S, Janda M, Cornish B, Battistutta D & Newman B. (2008). Lymphedema secondary to breast cancer: how choice of measure influences diagnosis, prevalence, and identifiable risk factors. *Lymphology* **41,** 18-28.

Mihara M, Hara H, Araki J, Kikuchi K, Narushima M, Yamamoto T, Iida T, Yoshimatsu H, Murai N, Mitsui K, Okitsu T & Koshima I. (2012). Indocyanine green (ICG) lymphography is superior to lymphoscintigraphy for diagnostic imaging of early lymphedema of the upper limbs. *PloS one* **7,** e38182.

Montgomery MK, Hallahan NL, Brown SH, Liu M, Mitchell TW, Cooney GJ & Turner N. (2013). Mouse strain-dependent variation in obesity and glucose homeostasis in response to high-fat feeding. *Diabetologia* **56,** 1129-1139.

Morrell RM, Halyard MY, Schild SE, Ali MS, Gunderson LL & Pockaj BA. (2005). Breast Cancer-Related Lymphedema. *Mayo Clinic Proceedings* **80,** 1480-1484.

Nelson TS, Akin RE, Weiler MJ, Kassis T, Kornuta JA & Dixon JB. (2014). Minimally invasive method for determining the effective lymphatic pumping pressure in rats using near-infrared imaging. *Am J Physiol Regul Integr Comp Physiol* **306,** 281-290.

Proulx ST, Luciani P, Alitalo A, Mumprecht V, Christiansen AJ, Huggenberger R, Leroux JC & Detmar M. (2013). Non-invasive dynamic near-infrared imaging and quantification of vascular leakage in vivo. *Angiogenesis* **16,** 525-540.

Rasmussen JC, Tan IC, Marshall MV, Fife CE & Sevick-Muraca EM. (2009). Lymphatic Imaging in Humans with Near-Infrared Fluorescence. *Current opinion in biotechnology* **20,** 74-82.

Savetsky IL, Torrisi JS, Cuzzone DA, Ghanta S, Albano NJ, Gardenier JC, Joseph WJ & Mehrara BJ. (2014). Obesity increases inflammation and impairs lymphatic function in a mouse model of lymphedema. *American Journal of Physiology - Heart and Circulatory Physiology* **307,** H165-H172.

Scallan JP & Huxley VH. (2010). In vivo determination of collecting lymphatic vessel permeability to albumin: a role for lymphatics in exchange. *The Journal of Physiology* **588,** 243-254.

Swartz MA, Kaipainen, A., Netti P. A., Brekken, C., & Boucher Y, Grodzinsky, A. J., Jain, R. K. (1999). Mechanics of interstitial-lymphatic fluid transport: theoretical foundation and experimental validation. *Journal of Biomechanics* **32,** 1297-1307.

Thomas-Maclean RL, Hack T, Kwan W, Towers A, Miedema B & Tilley A. (2008). Arm morbidity and disability after breast cancer: new directions for care. *Oncology nursing forum* **35,** 65-71.

Treves N. (1957). An evaluation of the etiological factors of lymphedema following radical mastectomy. An analysis of 1,007 cases. *Cancer* **10,** 444-459.

Unno N, Inuzuka K, Suzuki M, Yamamoto N, Sagara D, Nishiyama M & Konno H. (2007). Preliminary experience with a novel fluorescence lymphography using indocyanine green in patients with secondary lymphedema. *J Vasc Surg* **45,** 1016-1021.

Weiler M & Dixon JB. (2013). Differential transport function of lymphatic vessels in the rat tail model and the long-term effects of Indocyanine Green as assessed with near-infrared imaging. *Front Physiol* **4,** 215.

Weiler M, Kassis T & Dixon JB. (2012). Sensitivity analysis of near-infrared functional lymphatic imaging. *J Biomed Opt* **17,** 066019.